General Synthesis of Compound Semiconductor Nanowires**

By *Xiangfeng Duan* and *Charles M. Lieber**

The predictable synthesis of a broad range of multicomponent semiconductor nanowires has been accomplished using laser-assisted catalytic growth. Nanowires of binary group III–V materials (GaAs, GaP, InAs, and InP), ternary III–V materials (GaAs/P, InAs/P), binary II–VI compounds (ZnS, ZnSe, CdS, and CdSe), and binary SiGe alloys have been prepared in bulk quantities as high purity (>90 %) single crystals. The nanowires have diameters varying from three to tens of nanometers, and lengths extending to tens of micrometers. The synthesis of this wide range of technologically important semiconductor nanowires can be extended to many other materials and opens up significant opportunities in nanoscale science and technology.

The synthesis of nanoscale materials is critical to work directed towards understanding fundamental properties of small structures, creating nanostructured materials, and developing nanotechnologies.[1–5] Nanowires and nanotubes have been the focus of considerable attention because they have the potential to answer fundamental questions about one-dimensional systems and are expected to play a central role in applications ranging from molecular electronics to novel scanning microscopy probes.[2–5] To explore such diverse and exciting opportunities requires nanowire materials for which the chemical composition and diameter can be varied. Over the past several years considerable effort has been placed on the bulk synthesis of nanowires, and while advances have been made using template,[6] laser ablation,[7–9] solution,[10] and other[11] methods, in no case has it been demonstrated that one approach could be exploited in a predictive manner to synthesize a wide range of nanowire materials.[12] Here we describe the predictable synthesis of a broad range of binary and ternary III–V, II–VI, and IV–IV group semiconductor nanowires using the laser-assisted catalytic growth (LCG) method.

Recently, we reported the growth of elemental Si and Ge nanowires using the LCG method,[2,8] which exploits laser ablation to generate nanometer diameter catalytic clusters that define the size and direct the growth of the crystalline nanowires by a vapor–liquid–solid (VLS) mechanism.[2,4,8,13] A key feature of the VLS growth process and our LCG method is that equilibrium phase diagrams can be used to predict catalysts and growth conditions, thereby enabling rational synthesis of new nanowire materials. Significantly, we show here that semiconductor nanowires of the III–V materials GaAs, GaP, GaAsP, InAs, InP, InAsP, the II–VI materials ZnS, ZnSe, CdS, CdSe, and IV–IV alloys of SiGe can be synthesized in high yield and purity using this approach. Compound semiconductors, such as GaAs and CdSe, are especially intriguing targets since their direct bandgaps give rise to attractive optical and electrooptical properties. The nanowires have been prepared as single crystals with diameters as small as 3 nm, which places them in a regime of strong radial quantum confinement, and lengths exceeding 10 μm. These studies demonstrate that LCG represents a very general and predictive approach for nanowire synthesis, and moreover, we believe that the broad range of III–V, II–VI, and IV–IV nanowires prepared will open up many new opportunities in nanoscale research and technology.

The prediction of growth conditions for binary and more complex nanowires using the LCG method is, in principle, significantly more difficult than previous studies of elemental Si and Ge nanowires[2,4,8] due to the complexity of ternary and higher order phase diagrams. However, this complexity can be greatly reduced by considering pseudobinary phase diagrams for the catalyst and compound semiconductor of interest. For example, the pseudobinary phase diagram of Au–GaAs shows that Au–Ga–As liquid and GaAs solid are the principle phases above 630 °C in the GaAs rich region (Fig. 1).[14] This implies that Au can serve as a catalyst to grow GaAs nanowires by the LCG method, if

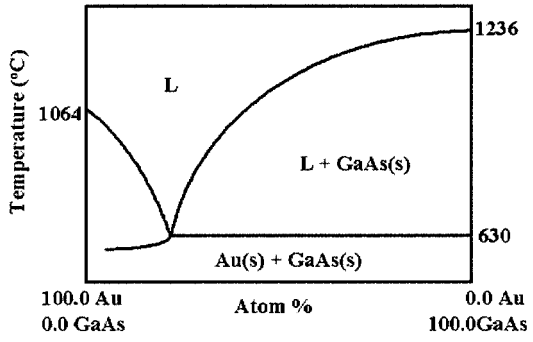

Fig. 1. Pseudobinary phase diagram for Au and GaAs. The liquid Au–Ga–As component is represented as L.

the target composition and growth temperature are set to this region of the phase diagram. Indeed, we find that LCG using $(GaAs)_{0.95}Au_{0.05}$ targets produces samples consisting primarily of nanowires. A typical field-emission scanning electron microscopy (FE-SEM) image of the material prepared at 890 °C (Fig. 2a) shows that the product is wire-like with lengths extending to 10 μm or more. Analyses of these high-resolution SEM images show that at least 90 % of the product produced by the LCG method is nanowire with only a small amount of particle material. X-ray diffraction (XRD) data from bulk samples can be indexed to the zinc blende (ZB) structure with a lattice constant consistent

[*] Prof. C. M. Lieber, X. Duan
Department of Chemistry and Chemical Biology
Harvard University
Cambridge, MA 02138 (USA)

[**] This work was supported by the Office of Naval Research (N00014-94-1-0302 and N00014-98-1-0499) and the National Science Foundation MRSEC (DMR-9809363). We acknowledge discussion with J. Hu, J.-L. Huang, L. Venkataraman, J. Wang, and Q. Wei, and thank M. Frongillo and Y. Lu for help with TEM.

  0935-9648/00/0402-0298 $ 17.50+.50/0

ADVANCED MATERIALS

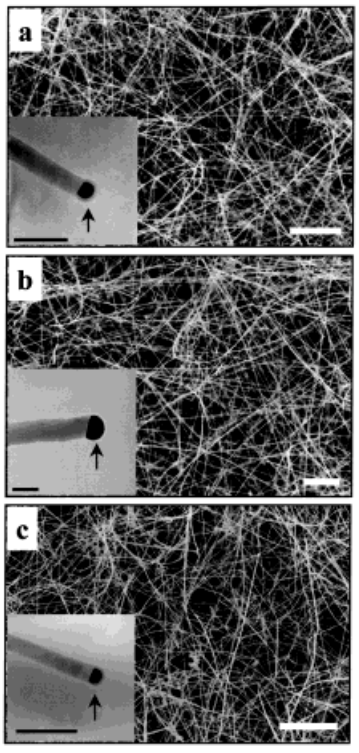

Fig. 2. FE-SEM images of a) GaAs, b) GaP, and c) $GaAs_{0.6}P_{0.4}$ nanowires prepared by LCG (the scale bars are 2 μm). The respective insets are TEM images of GaAs, GaP, and $GaAs_{0.6}P_{0.4}$ nanowires (the scale bars are all 50 nm). The high contrast (dark) features correspond to the solidified nanocluster catalysts.

with bulk GaAs, and also show that the material is pure GaAs to the 1 % level. Lastly, we note that high yields of GaAs nanowires were also obtained using Ag and Cu catalysts. These data are consistent with the fact that these metals (M = Ag, Cu) exhibit M–Ga–As liquid and GaAs solid phase in the GaAs rich regions of the psuedobinary phase diagrams,[14] and furthermore, demonstrate the predictability of the LCG approach to nanowire growth.

The structure and composition of the GaAs nanowires have been characterized in detail using transmission electron microscopy (TEM), convergent beam electron diffraction (ED), and energy dispersive X-ray fluorescence (EDX). TEM studies show that the nanowires have diameters ranging from 3 nm to ca. 30 nm. A typical diffraction contrast image of a single 20 nm diameter wire (Fig. 3a) indicates that the wire is single crystal (uniform contrast) and uniform in diameter. The Ga:As composition of this wire determined by EDX, 51.4:48.6, is the same as the composition obtained from analysis of a GaAs crystal standard, within limits of instrument sensitivity. Moreover, the ED pattern recorded perpendicular to the long axis of this nanowire (inset, Fig. 3a) can be indexed for the (112) zone axis of the ZB GaAs structure, and thus shows that growth occurs along the (111) direction. Extensive measurements of individual GaAs nanowires show that growth occurs along the (111) directions in all cases. This direction and the single crystal structure are further confirmed by lattice-resolved TEM images (e.g., Fig. 3b) that show clearly the (111) lattice planes (spacing 0.32 ± 0.01 nm; bulk GaAs, 0.326 nm) perpendicular to the wire axis. Lastly, the TEM studies reveal that most nanowires terminate at one end with a nanoparticle (inset, Fig. 2a). EDX analysis indicates that the nanoparticles are composed mainly of Au. The presence of Au nanoparticles at the ends of the nanowires is consistent with the pseudobinary phase diagram, and represents strong evidence for a VLS growth mechanism proposed for LCG.

The successful synthesis of binary GaAs nanowires by LCG is not an isolated case but general to a broad range of binary and more complex nanowire materials (Table 1). To extend our synthetic approach to the broadest range of nanowires, we recognize that catalysts for LCG can be chosen in the absence of detailed phase diagrams by identifying metals in which the nanowire component elements are soluble in the liquid phase but that do not form solid compounds more stable than the desired nanowire phase; i.e., the ideal metal catalyst should be physically active but chemically stable. From this perspective the noble metal Au should represent a good starting point for many materials. This noble metal also has been used in the past for the VLS growth of surface supported nanowires by metal-organic chemical vapor deposition (MOCVD).[15] The nanowires produced by the MOCVD method are distinct from

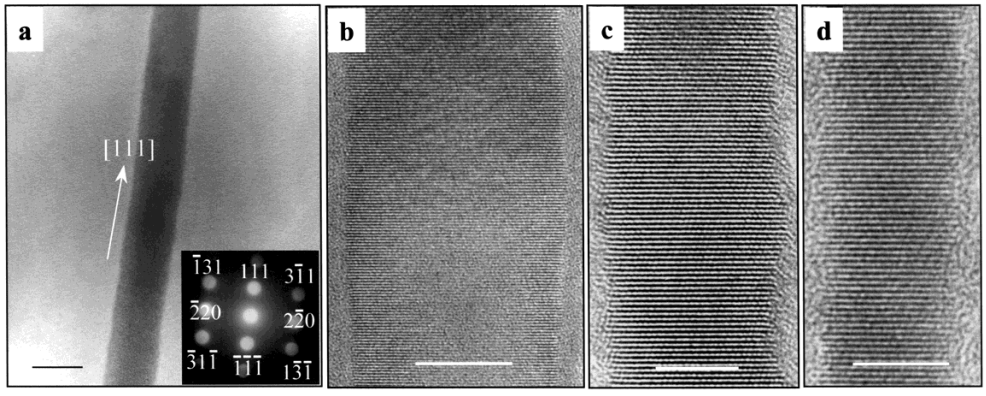

Fig. 3. a) Diffraction contrast TEM image of a ca. 20 nm diameter GaAs nanowire. The inset shows a convergent beam electron diffraction pattern (ED) recorded along the (112) zone axis. The (111) direction of the ED pattern is parallel to the wire axis, and thus shows that growth occurs along the (111) direction. The scale bar corresponds to 20 nm. b) High-resolution TEM image of a ca. 20 nm diameter GaAs nanowire. The lattice spacing perpendicular to the nanowire axis, 0.32 ± 0.01 nm, is in good agreement with the 0.326 nm spacing of (111) planes in bulk GaAs. The scale bar corresponds to 10 nm. c) and d) High-resolution TEM images of respectively 10 and 6 nm diameter $GaAs_{0.6}P_{0.4}$ nanowires. The (111) lattice planes (perpendicular to the wire axes) are clearly resolved in both nanowires. The scale bars in (b) and (c) are 5 nm.

  0935-9648/00/0402-0299 $ 17.50+.50/0

the materials reported in this communication in several regards, including 1) the MOCVD nanowires are produced on surfaces and not in the bulk quantities required for assembly, 2) the MOCVD nanowires taper significantly from the base to their ends (that is, they do not have uniform diameters), and 3) the smallest nanowire diameters, 10–15 nm, are significantly larger than the 3–5 nm diameters achieved in our work. Lastly, as described below, it is important to recognize that our LCG method is readily extended to many different materials (Table 1) simply by producing solid targets of the material of interest and catalyst.

Table 1. Summary of single crystal nanowires synthesized. The growth temperatures correspond to ranges explored in these studies. The minimum and average nanowire diameters were determined from TEM and FE-SEM images. Structures were determined using electron diffraction and lattice resolved TEM imaging: ZB, zinc blende; W, wurtzite; and D, diamond structure types. Compositions were determined from EDX measurements made on individual nanowires. All of the nanowires were synthesized using Au as the catalyst, except GaAs, for which Ag and Cu were also used. The GaAs nanowires obtained with Ag and Cu catalysts have the same size distribution, structure, and composition as those obtained with the Au catalyst.

Material	Growth Temperature [°C]	Minimum Diameter [nm]	Average Diameter [nm]	Structure	Growth Direction	Ratio of Components
GaAs	800–1030	3	19	ZB	<111>	1.00 : 0.97
GaP	870–900	3–5	26	ZB	<111>	1.00 : 0.98
$GaAs_{0.6}P_{0.4}$	800–900	4	18	ZB	<111>	1.00 : 0.58 : 0.41
InP	790–830	3–5	25	ZB	<111>	1.00 : 0.98
InAs	700–800	3–5	11	ZB	<111>	1.00 : 1.19
$InAs_{0.5}P_{0.5}$	780–900	3–5	20	ZB	<111>	1.00 : 0.51 : 0.51
ZnS	990–1050	4–6	30	ZB	<111>	1.00 : 1.08
ZnSe	900–950	3–5	19	ZB	<111>	1.00 : 1.01
CdS	790–870	3–5	20	W	<100>, <002>	1.00 : 1.04
CdSe	680–1000	3–5	16	W	<110>	1.00 : 0.99
$Si_{1-x}Ge_x$	820–1150	3–5	18	D	<111>	$Si_{1-x}Ge_x$

First, we have extended significantly our work on GaAs to include GaP and ternary alloys $GaAs_{1-x}P_x$. FE-SEM images of the product obtained by LCG from $(GaP)_{0.95}Au_{0.05}$ targets reveal high-purity nanowires with lengths exceeding 10 μm (Fig. 2b). Extensive TEM characterization shows that these nanowires i) are single crystal GaP, ii) grow along the (111) directions, and iii) terminate in Au nanoparticles (inset, Fig. 2b) as expected for the LCG mechanism. We have further tested the limits of our LCG approach through studies of ternary GaAsP alloy nanowires. The synthesis of ternary III–V alloys is of particular interest for bandgap engineering, which is critical for electronic and optical devices.[16] LCG of GaAsP nanowires using a $GaAs_{0.6}P_{0.4}$ target with a Au catalyst yielded nearly pure nanowires (Fig. 2c). TEM images, ED, and EDX show that these nanowires are single crystals, grow along the (111) directions, have a Ga:As:P ratio, 1.0:0.58:0.41, that is essentially the same as the starting target composition, and terminate in nanoclusters that are composed primarily of Au (inset, Fig 2c). High-resolution TEM images recorded on nanowires with diameters of ca. 10 and 6 nm (Fig. 3c and 3d) show well-ordered (111) lattice planes and no evidence for compositional modulation. The observation that the ternary nanowire composition can be controlled by target composition is especially important, because it provides an opportunity to explore exciton energy changes due to both bandgap variations (composition) and quantum confinement (size).

Based on the above results, it is perhaps not surprising that we have also successfully used LCG to prepare III–V binary and ternary materials containing In–As–P (Table 1). A more significant point is that this synthetic approach can also be easily extended to the preparation of many other classes of nanowires, including the II–VI materials ZnS, ZnSe, CdS, CdSe (Table 1), and IV–IV SiGe alloys. The cases of the II–VI nanowires CdS and CdSe are especially important, because a stable structural phase of these materials, wurtzite (W), is distinct from the ZB structure of the III–V materials described above and the ZB structure of ZnS and ZnSe.[17,18] Significantly, we find that nanowires of CdS and CdSe can be synthesized in high yield using the LCG approach with an Au catalyst (Fig. 4a). TEM and ED data obtained on individual CdSe nanowires (for example, Fig. 4b and 4c) demonstrate that these materials are single crystals with a W-type structure and (110) growth direction that is clearly distinguished from the (111) direction of ZB structures. Studies of CdS nanowires (Table 1) show somewhat more complex behavior; that is, W-type nanowires with growth along two distinct (100) and (002) directions. It is possible that the (002) direction assigned for a minority of CdS nanowires could correspond to the (111) direction of a ZB structure. However, XRD measurements made on bulk nanowire samples are consistent with the W assignment. In addition, previous studies of W-type CdS and CdSe nanoclusters showed elongation along the (002) direction.[18] We believe that systematic studies of the nanowire structure as a function of growth temperature should help to elucidate the origin of these results for CdS, and could also provide insight into how nanowire growth direction might be controlled.

Lastly, we have used LCG to prepare nanowires of IV–IV binary Si–Ge alloys (Table 1). Using an Au catalyst, it was possible to synthesize single crystal nanowires over the entire $Si_{1-x}Ge_x$ composition range. Unlike the case of GaAsP discussed above, the Si–Ge alloys do not exhibit the same compositions as the starting targets. Rather, the composition varies continuously within the growth reactor with Si-rich materials produced in the hotter central region and Ge-rich materials produced at the cooler end. Specifically, LCG growth from a $(Si_{0.70}Ge_{0.30})_{0.95}Au_{0.05}$ target at 1150 °C produced nanowires with a Si:Ge ratio of 95:5, 81:19, 74:26,

  0935-9648/00/0402-0300 $ 17.50+.50/0

ADVANCED MATERIALS

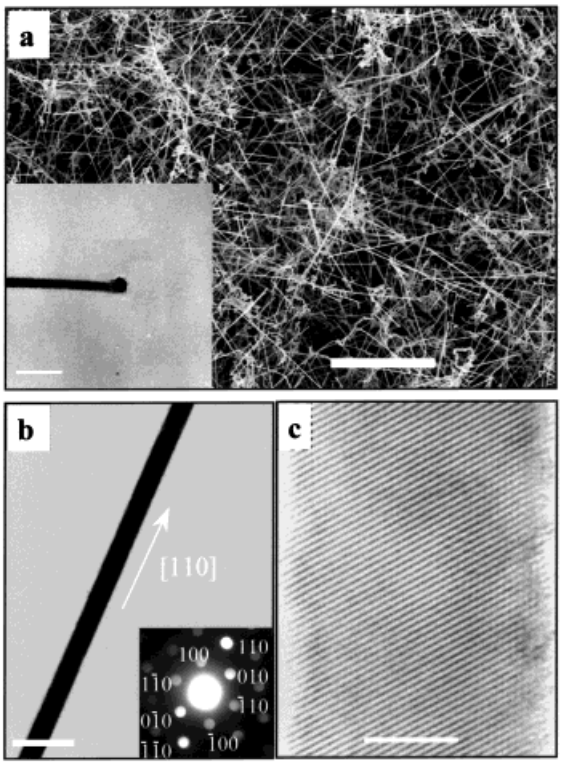

Fig. 4. a) FE-SEM image of CdSe nanowires prepared by LCG. The scale bar corresponds to 2 μm. The inset is the TEM image of an individual CdSe nanowire exhibiting nanocluster (dark feature) at the wire end. EDX shows that the nanocluster is composed primarily of Au. The scale bar is 50 nm. b) Diffraction contrast TEM image of an 18 nm diameter CdSe nanowire. The uniform contrast indicates that the nanowire is single crystal. The inset is the ED pattern, which has been indexed to the wurtzite structure, recorded along the (001) zone axis. The (110) direction of the ED pattern is parallel to the wire axis, and thus shows that growth occurs along the (110) direction. The scale bar is 50 nm. c) High-resolution TEM image of a ca. 13 nm diameter CdSe nanowire exhibiting well-resolved (100) lattice planes. The experimental lattice spacing, 0.36 ± 0.01 nm, is consistent with the 0.372 nm separation in bulk crystals. The 30° orientation (100) lattice planes with respect to the nanowire axis is consistent with the (110) growth direction determined by ED. The scale bar corresponds to 5 nm.

34:66, and 13:87 from the furnace center to end, respectively. This composition variation arises from the fact that the optimal growth temperatures of the two individual nanowire materials are quite different. Such differences can increase the difficulty in synthesizing controlled composition alloys, although our results also show that this can be exploited to prepare a range of alloy compositions in a single growth experiment.

In conclusion, we have synthesized a wide range of single-crystal binary and ternary compound semiconductor nanowires using our LCG technique. These results clearly demonstrate the generality of this approach for rational nanowire synthesis. The availability of these high-quality, single-crystal semiconductor nanowires is expected to enable fascinating opportunities in nanometer scale science and technology. For example, these nanowires can be used to probe the confinement, dynamics, and transport of excitons in 1D,[5,19] and can serve as optically-active building blocks for nanostructured materials. Moreover, by further controlling growth, we believe that our LCG approach can be used to synthesize more complex nanowire structures, including single-wire homo- and heterojunctions,[20] and superlattices, and thus may enable the synthesis of nanoscale light-emitting diodes and laser devices.

Experimental

The apparatus and general procedures for LCG growth of nanowires have been described previously [2,4,8]. The targets used in syntheses consisted of $(material)_{0.95}Au_{0.05}$. Typical conditions used for synthesis were i) 100–500 torr Ar:H_2 (95:5), ii) 50–150 sscm gas flow, and iii) ablation with a pulsed Nd:YAG laser (λ = 1064 nm; 10 Hz pulse rate; 2.5 W average power). Specific temperatures used for the growth of different nanowire materials are given in Table 1. The nanowire products were collected at the down-stream cold end of the furnace.

The nanowire samples were characterized using XRD (SCINTAG XDS 2000), FE-SEM (LEO 982), and TEM (Philips 420 and JEOL 2010). Electron diffraction and composition analysis (EDX) measurements were also made on the TEMs. Samples for TEM analysis were prepared as follows: samples were briefly sonicated in ethanol, which suspended the nanowire material, and then a drop of suspension was placed on a TEM grid and allowed to dry.

Received: August 30, 1999
Final version: November 11, 1999

[1] a) L. E. Brus, *J. Phys. Chem.* **1994**, *98*, 3575. b) C. B. Murray, C. R. Kagan, M. G. Bawendi, *Science* **1995**, *270*, 1335. c) A. P. Alivisatos, *Science* **1996**, *271, 933. d) C. P. Collier, T. Vossmeyer, J. R. Heath, Annu. Rev. Phys. Chem.* **1998**, *49*, 371.
[2] a) C. M. Lieber, A. M. Morales, P. E. Sheehan, E. W. Wong, P. Yang, in *Proceedings of the Robert A. Welch Foundation 40th Conference on Chemical Research: Chemistry on the Nanometer Scale*, R. A. Welch Foundation, Houston **1997**, pp. 165–187. b) C. M. Lieber, *Solid State Commun.* **1998**, *107, 106*.
[3] a) B. I. Yacobson, R. E. Smalley, *Am. Sci.* **1997**, *85, 324. b) C. Dekker, Phys. Today* **1999**, *52*, 22.
[4] J. Hu, T. W. Odom, C. M. Lieber, *Acc. Chem. Res.* **1999**, *32*, 435.
[5] D. Snoke, *Science* **1996**, *273, 1351.*
[6] a) C. R. Martin, *Science* **1994**, *266*, 1961. b) J. C. Hulteen, C. R. Martin, *J. Mater. Chem.* **1997**, *7*, 1075. c) H. Dai, E. W. Wong, Y. Z. Lu, S. Fan, C. M. Lieber, *Nature* **1995**, *375*, 769. d) W. Han, S. Fan, W. Li, Y. Hu, *Science* **1997**, *277*, 1287.
[7] a) A. Thess, R. Lee, P. Nikolaev, H. Dai, P. Petit, J. Robert, C. H. Xu, Y. H. Lee, S. G. Kim, A. G. Rinzler, D. T. Colbert, G. E. Scuseria, D. Tomanek, J. E. Fischer, R. E. Smalley, *Science* **1999**, *271*, 483. b) Y. Zhang, K. Suenaga, C. Colliex, S. Iijima, *Science* **1998**, *281*, 973.
[8] A. M. Morales, C. M. Lieber, *Science* **1998**, *279*, 208.
[9] D. P. Yu, C. S. Lee, I. Bello, X. S. Sun, Y. H. Tang, G. W. Zhou, Z. G. Bai, Z. Zhang, S. Q. Feng, *Solid State Commun.* **1998**, *105*, 403.
[10] a) T. J. Trentler, K. M. Hickman, S. C. Goel, A. M. Viano, P. C. Gibbons, W. E. Buhro, *Science* **1995**, *270*, 1791. b) T. J. Trentler, S. C. Goel, K. M. Hickman, A. M. Viano, M. Y. Chiang, A. M. Beatty, P. C. Gibbons, W. E. Buhro, *J. Am. Chem. Soc.* **1997**, *119*, 2172. c) S.-S. Chang, C.-W. Shih, C.-D. Chen, W.-C. Lai, C. R. C. Wang, *Langmuir* **1999**, *15*, 701. d) Y. Li, Y. Ding, Z. Wang, *Adv. Mater.* **1999**, *11*, 847.
[11] a) P. Yang, C. M. Lieber, *Science* **1996**, *273*, 1836. b) P. Yang, C. M. Lieber, *J. Mater. Res.* **1997**, *12*, 2981. c) Y. Q. Zhu, W. B. Hu, W. K. Hsu, M. Terrones, N. Grobert, T. Karali, H. Terrones, J. P. Hare, P. D. Townsend, H. W. Kroto, D. R. Walton, *Adv. Mater.* **1999**, *11*, 844.
[12] Template mediated methods using membranes and nanotubes have been used to prepare a number of materials. However, these nanowires typically have diameters >10 nm, which are larger than those desired for strong quantum confinement effects, and often have polycrystalline structures that make it difficult to probe intrinsic physical properties.
[13] R. S. Wagner, W. C. Ellis, *Appl. Phys. Lett.* **1964**, *4*, 89.
[14] M. B. Panish, *J. Electrochem. Soc.* **1969**, *114*, 517.
[15] a) K. Hiruma, M. Yazawa, T. Katsuyama, K. Ogawa, K. Haraguchi, M. Koguchi, H. Kakibayashi, *J. Appl. Phys.* **1995**, *77*, 447. b) T. Shimada, K. Hiruma, M. Shirai, M. Yazawa, K. Haraguchi, T. Sato, M. Matsui, T. Katsuyama, *Superlattices Microstruct.* **1998**, *24*, 453.

  0935-9648/00/0402-0301 $ 17.50+.50/0

[16] For example, see: F. Capasso, A. Y. Cho, *Surf. Sci.* **1994**, *299*, 878.
[17] L. I. Berger, *Semiconductor Materials*, CRC Press, Boca Raton, FL **1997**, pp. 198–203.
[18] C. B. Murray, D. J. Norris, M. G. Bawendi, *J. Am. Chem. Soc.* **1993**, *115*, 8706.
[19] H. Akiyama, *J. Phys.: Condens. Matter* **1998**, *10*, 3095.
[20] J. Hu, M. Ouyang, P. Yang, C. M. Lieber, *Nature* **1999**, *399*, 48.

Topotactic Release of CdS and $Cd_{1-x}Mn_xS$ from Solid Thioalkanoates with Ammonia to Yield Quantum Particles Arranged in Layers Within an Organic Composite**

By *Shouwu Guo*, *Leandro Konopny*, *Ronit Popovitz-Biro*, *Hagai Cohen*, *Marina Sirota*, *Efrat Lifshitz*, and *Meir Lahav**

Dedicated to Prof. D. Möbius on the occasion of his 60th birthday

In recent years there has been an interest in the preparation of hybrid organic/inorganic composite materials, where the inorganic components are of quantum-size and arranged in periodic patterns within the organic matrices. Such materials are anticipated to express unique opto-electronic properties, differing from composites where the particles are randomly distributed.[1–9] Recently we followed a two-step synthetic methodology for the preparation of such materials. In the first step we select or design organometallic solids in the form of 3D crystals or Langmuir–Blodgett (LB) films where the metal ions are arranged in layers or other patterns. These phases are transformed, in a second step, by a topotactic gas/solid reaction into organic/inorganic composites, where the inorganic components are semiconductor quantum particles. The latter are arranged in layers that preserve, at least partially, the periodic order of the ions in the reactant matrix. This approach was applied to the preparation of CdS and PbS nanoparticle patterns within alkanoic acids.[10–12] Here we describe a new synthetic route to the preparation of such composites. The method comprises the release of metal sulfide particles, at specific sites of the solid, from the corresponding crystalline thioalkanoate salts with gaseous ammonia. The organization of the particles is improved in some systems and induced in others by using Cd alkanoates as site-directing nucleating centers.

Salts of metal thioalkanoates, such as Cd, Pb, Hg, and Mn, crystallize into 3D crystals, in which the metal ions form layers separated from one another by a bilayer of the thioalkanoates. In fact, one may control the spacing between these ion layers by selecting a thioalkanoic acid with the appropriate chain length. Reaction of these solid salts with a gaseous nucleophile such as ammonia should result in the release of metal sulfide molecules at hydrophilic sites of the salt while converting the thioalkanoates into the corresponding amides.

Pure salts of Cd thioalkanoates $[CH_3(CH_2)_nCOS]_2Cd$ (n = 10 to 24) were prepared from the corresponding potassium salts. X-ray powder diffraction (XRD) measurements show that the thioalkanoates crystallize in bilayer structures and the d-spacing between the ion layers is determined by the length of the hydrocarbon chains (34.27 Å for the n = 10 system, 42.43 Å for n = 14, 46.50 Å for n = 16, 56.35 Å for n = 20, 65.40 Å for n = 24). Crystalline powders of Cd thioalkanoates with n = 10 to 24 were exposed to dry ammonia in a sealed dessicator at atmospheric pressure and room temperature. The reactions were complete within two to four days, yielding CdS and the corresponding alkylamide, as suggested in Equations 1 and 2.[13]

$$[CH_3(CH_2)_nCOS]_2Cd + 3\,NH_3 \longrightarrow [Cd(SH)_2] + CH_3(CH_2)_nCONH_2 \quad (1)$$

$$[Cd(SH)_2] \longrightarrow CdS + [H_2S] \quad (2)$$

Figures 1a–e show transmission electron microscopy (TEM) images of the solid composites of n = 14, 16, 20, 24, and 10, respectively. In systems with n = 10 and 14, the particles are spheres of 50 to 60 Å in diameter that are randomly distributed within the organic matrix, whereas in systems of n = 16, 20, and 24, the particles are elongated, 60–70 Å long and 15–20 Å wide, and arranged in periodic layers within the organic matrices. The d-spacings of 3.36 Å (111), 2.06 Å (220), and 1.76 Å (311), determined by XRD and electron diffraction (ED) patterns, demonstrated that the CdS particles are of the cubic form. The size of the particles was also preserved after suspending the reacted crystallites in toluene. Figure 2A shows the UV-vis absorption spectra of the CdS particles formed within n = 14 to 24 thioalkanoates after being suspended in toluene. The particle sizes deduced from these spectra are in agreement with those determined by TEM.

The present experiments demonstrate that, in order for the nanoparticles to crystallize at the hydrophilic sites of the matrix, the spacing between the ion layers within the reactant should be beyond 45 Å. The probability that these particles nucleate site-selectively can be increased by introducing Cd alkanoates as site-directing nucleation auxiliaries. Within these mixed crystals, Cd ions should be bound to two thiocarboxylate groups (pair I), as in the pure

[*] Prof. M. Lahav, S. Guo, Dr. L. Konopny, Dr. R. Popovitz-Biro
Department of Materials and Interfaces
Weizmann Institute of Science
76100 Rehovot (Israel)
Dr. H. Cohen
Chemical Service Unit
Weizmann Institute of Science
76100 Rehovot (Israel)
Prof. E. Lifshitz, M. Sirota
Department of Chemistry and Solid State Institute
Technion
32000 Haifa (Israel)

[**] This work was supported by the Israel Ministry of Science and the Petroleum Research Funds of the American Chemical Society. LK thanks the Campomar Foundation (Argentina) and G. M. J. Schmidt Minerva Center for a fellowship. We thank Ms. Edna Shavit for the synthesis of thioalkanoic acids and Ms. Jingyan Zhang for performing the EPR measurements.

  0935-9648/00/0402-0302 $ 17.50+.50/0